RSC Advances

PAPER

View Article Online
View Journal | View Issue

Cite this: *RSC Adv.*, 2024, **14**, 5609

Cobalt-modulated dual emission carbon dots for ratiometric fluorescent vancomycin detection†

Khalid Alhazzani,[a] Ahmed Z. Alanazi,[a] Aya M. Mostafa,[bc] James Barker,[b] Mohamed M. El-Wekil[c] and Al-Montaser Bellah H. Ali *[c]

Received 27th December 2023
Accepted 7th February 2024

DOI: 10.1039/d3ra08899e

rsc.li/rsc-advances

This work presents a simple yet selective fluorometric protocol for the quantification of vancomycin, an important antibiotic for treating infections caused by Gram-positive bacteria. A novel ratiometric fluorometric method for the determination of vancomycin is developed based on dual emissive carbon dots (DECDs) with emission at 382 nm and 570 nm in combination with Co^{2+} ions. Upon addition of Co^{2+}ions, the fluorescence at 382 nm of DECDs is enhanced while emission at 570 nm remains constant. In the presence of vancomycin, it complexes with Co^{2+} leading to quenching of the 382 nm fluorescence due to strong binding with Co^{2+} in the Co@DECDs system. The DECDs are fully characterized by TEM and different spectroscopic techniques. The proposed ratiometric method is based on measuring fluorescence ratio (F_{570}/F_{382}) against vancomycin concentration and the method exhibits a good linearity range from 0.0 to 120.0 ng mL^{-1} with a low limit of detection (S/N = 3) of 0.31 ng mL^{-1}. The method shows good selectivity with minimal interference from potential interfering species. This ratiometric fluorometric approach provides a promising tool for sensitive and specific vancomycin detection in clinical applications.

1. Introduction

Vancomycin is a glycopeptide antibiotic that is often used in the prophylaxis and therapy against infections by many Gram-positive bacteria, including methicillin-resistant staphylococci.[1] It exerts its antibacterial effects through multiple mechanisms, including inhibiting peptidoglycan synthesis, altering cell membrane permeability, and interfering with RNA synthesis in the cytoplasm.[2] The absorption of vancomycin in the digestive tract is poor, and intramuscular injection can lead to severe local pain and tissue damage. It is typically administered intravenously using 5% dextrose or 0.9% saline solutions.[3] After administration, vancomycin quickly distributes to various body tissues, achieving therapeutic concentrations in the lungs, heart, synovial fluid, peritoneal fluid, bone, and kidneys.[4] In patients with normal kidney function, more than 90% of the drug is excreted unchanged through the kidneys. Several factors, including age, body weight, serum albumin levels, and concurrent medications, can influence the pharmacokinetics of vancomycin.[4] Vancomycin is administrated intravenously and has a half-life of 6–12 h and binds to plasma proteins by 10–50%.[5] The recommended target trough concentration range for vancomycin is 10–15 mg L^{-1}. To prevent the development of bacterial resistance, the minimum trough concentration should exceed 10 mg L^{-1} (6.9 μmol L^{-1}).[6] Vancomycin has a narrow therapeutic window, where concentrations above the effective level can become toxic. Insufficient drug concentrations can lead to the development of bacterial resistance,[7] while excessively high concentrations can cause adverse effects such as nephrotoxicity, ototoxicity, hypotension, phlebitis, hypersensitivity reactions, red man syndrome, neutropenia, chills, fever, and interstitial nephritis.[2] Therefore, therapeutic drug monitoring of vancomycin is necessary. Various analytical methods, including high performance liquid chromatography (HPLC),[8–10] electrochemical detection,[11,12] immunoassay,[13,14] UV-vis spectrophotometric[15,16] and fluorometric methods[17–23] have been employed to quantify vancomycin in biological samples.

Carbon dots (CDs) are a new class of carbon-based nanomaterials that have recently attracted tremendous attention due to their intriguing properties and advantages.[24,25] CDs are small carbon nanoparticles with dimensions below 10 nm.[26] Compared to traditional semiconductor quantum dots, CDs exhibit superior optical properties, excellent biocompatibility, low toxicity, and environmental friendliness.[27] These features make them highly promising materials for a variety of applications including sensing, bioimaging, photocatalysis, and optoelectronic devices.[27] There are several methods available for synthesizing CDs, both top-down and bottom-up approaches. Top-down methods involve

[a]*Department of Pharmacology and Toxicology, College of Pharmacy, King Saud University, Riyadh, Saudi Arabia*

[b]*School of Life Sciences, Pharmacy, and Chemistry, Kingston University, Kingston-upon-Thames, London KT1 2EE, UK*

[c]*Department of Pharmaceutical Analytical Chemistry, Faculty of Pharmacy, Assiut University, Assiut, Egypt. E-mail: Almontaser_bellah@aun.edu.eg*

† Electronic supplementary information (ESI) available. See DOI: https://doi.org/10.1039/d3ra08899e

breaking down carbon-based precursors like carbon nanotubes or graphite using electrochemical oxidation, laser ablation, arc discharge, or chemical oxidation.[26,28,29] Bottom-up methods build up CDs from molecular precursors using hydrothermal treatment, microwave synthesis, ultrasonic synthesis, or thermal decomposition.[30] Additional post-treatment steps like surface passivation are often utilized to enhance the CDs' photoluminescence.[31–33] Functionalizing CDs by incorporating other atoms, especially transition metals, allows fine-tuning of their optoelectronic properties. Transition metals can be coordinated to ligands on the CD surface, introducing new energy levels that modify light absorption and emission intensities or wavelengths.[32] Among various metals, Co^{2+} shows particular promise for enhancing CD performance.[34–37] Co^{2+} ions can interact with carbon dots through Co^{2+} centers and CD π-conjugated framework. The coordination complexes that may be formed between Co^{2+} and CD surface groups like nitrogen or oxygen can lead to enhancement in fluorescence intensity.

Dual emissive carbon dots (DECDs) were synthesized *via* a facile one-step hydrothermal method using aconitic acid and 4-dimethylaminobenzaldehyde as precursors. The as-prepared DECDs exhibited distinct dual fluorescence emission peaks centered at 382 nm and 570 nm, corresponding to the respective electron transition behaviors of the carbon core and surface states.[38,39] Concurrent incorporation of Co^{2+} ions resulted in significantly enhanced fluorescence intensity of the 382 nm peak, attributed to synergetic effects between the cobalt ions and the carbon nanodot framework. The longer wavelength emission peak at 570 nm remained unaffected by the presence of cobalt. The dual emissive nature of the Co^{2+}-dual emissive carbon dots (Co@DECDs) system allowed exploration of ratiometric detection strategies. Herein, a turn-off ratiometric sensor based on Co@DECDs system for selective analysis of the glycopeptide antibiotic vancomycin is developed. Upon addition of vancomycin samples, the shorter wavelength fluorescence peak at 382 nm demonstrated notable quenching due to specific chelation interactions between vancomycin and the Co^{2+} ions. Simultaneously, the 570 nm emission peak remained constant without interference from vancomycin addition. By monitoring changes in the relative peak intensity ratio (F_{570}/F_{382}) after vancomycin introduction, sensitive ratiometric quantification could be achieved. The unique dual emissions thus enabled reliable determination of vancomycin concentration in spiked human plasma samples, with good sensitivity and reliability.

2. Experimental

2.1 Materials

Vancomycin (Assay 99.9%) pure powder was obtained as a gift from Egy pharma (Nasr City, Cairo, Egypt). Aconitic acid, 4-dimethylaminobenzaldehyde, phosphoric acid, acetic acid, boric acid, sodium hydroxide, cobalt chloride, and quinine sulfate were purchased from Sigma Aldrich (Steinheim, Germany). All chemicals and reagents were of analytical reagent grade and were used as received without further purification. Double distilled water was purified using a Milli-Q Plus Water Purification System (Millipore, Billerica, MA, USA).

2.2 Instrumentation

Spectrofluorometer (Shimadzu RF-5301 PC, Japan) was used to record the fluorescence spectra. UV-vis absorption spectra were monitored using the UV-vis spectrophotometer (UV-1601; Shimadzu, Japan). FT-IR (Fourier transform infrared spectrophotometer) was recorded using nicolet 6700 spectrometer (Thermo Electron Corporation, USA). TEM (Transmission Electron Microscopy) images were taken using TEM, JEM-1400, Japan. XRD (X-ray diffraction) patterns were obtained on a Philips PW 1710 diffractometer (Eindhoven, Netherlands), where the tube anode was Cu with $K_\alpha = 1.54242$ Å.

2.3 Preparation of Co@DECDs system

Dual emissive carbon dots (DECDs) were prepared through a hydrothermal process by dissolving 0.5 g aconitic acid and 0.5 g 4-dimethylaminobenzaldehyde in 30 mL of deionized water. The precursors were placed in a Teflon-lined stainless-steel autoclave and heated to 180 °C for 8 h. Upon cooling the autoclave to room temperature, the obtained pale-yellow solution was separated from larger particles by centrifugation at $7155 \times g$ for 20 minutes. The collected supernatant was then dialyzed for 24.0 h across a 500 MWCO membrane against 1.5 L distilled water. The purified carbon dots were lyophilized to obtain a dry powder which was then resuspended in deionized water to prepare a concentration of 10 mg mL^{-1} for further experiments and characterization. The Co@DECDs system was prepared by adding 1 mL of a 1.0 mg mL^{-1} cobalt chloride solution to 1 mL of the 10 mg mL^{-1} lyophilized DECDs and diluting to 10 mL total volume with distilled water.

2.4 Vancomycin determination by Co@DECDs system

At room temperature, the fluorescence emission intensity of the prepared Co@DECDs at 382 nm and 570 nm as the blank sample excited by light at 270 nm was measured. To 100.0 μL of Co@DECDs, serial concentrations of vancomycin (1 mL, 0–1200 ng mL^{-1}) were transferred to a set of 10.0 mL volumetric flasks using Britton–Robinson buffer (0.02 M) with pH of 7.0, mixed well and allowed to equilibrate for 1 min. After 1 min, the fluorescent intensity ratio (F_{570}/F_{382}) of the samples were measured. By plotting fluorescence intensity ratio (F_{570}/F_{382}) against the final concentration of vancomycin, calibration curves were created.

2.5 Analysis of vancomycin in spiked human plasma

To a set of centrifugation tubes, accurately measured volumes of human plasma (0.5 mL) were transferred and then spiked with different aliquots of vancomycin stock solution. The solutions were mixed with vortex for 5 min, completed to 5.0 mL with methanol for complete protein precipitation and then centrifuged at $1790 \times g$ for 15 min. The upper layers were aspirated and filtered. After that, accurate volumes (constant volume of 1.0 mL) of the filtrate were transferred to a set of 10 mL volumetric flasks and completed with methanol to obtain final concentrations in the range of 0.0–120.0 ng mL^{-1}. A blank plasma experiment was prepared simultaneously.

2.6 Fluorescence quantum yields (QYs) of DECDs

For detailed procedures, please refer to the ESI.†

3. Results and discussion

3.1 Structural and morphological characterization

The transmission electron microscopy was used to examine the structures of the prepared DECDs. The results depicted in Fig. 1A illustrate that the DECDs exhibited a uniform spherical shape and were evenly dispersed in the aqueous solution. The size distribution of the particles was relatively narrow, with diameters ranging from 2 to 9 nm, and the average diameter was measured to be 3.4 nm (inset of Fig. 1A). The amorphous nature of the DECDs was confirmed by analyzing their X-ray diffraction (XRD) pattern (Fig. 1B), which exhibited two broad diffraction peaks at approximately 20° and 30°.

The FT-IR spectrum of the DECDs exhibits distinctive peaks indicative of the chemical functionalities present in the carbon dot structure (Fig. 1C). The broad peak at 3422 cm^{-1} suggests the presence of O–H/N–H stretching vibrations.[28,29,40] The shoulder peak at 2932 cm^{-1} corresponds to C–H stretching vibrations, signifying the presence of aliphatic hydrocarbons. The small broad peak at 2360 cm^{-1} may be associated with C≡N stretching vibrations. The peak at 1633 cm^{-1} is attributed to C=O stretching vibrations.[41] The peak at 1160 cm^{-1} corresponds to C–O stretching vibrations. The peak at 998 cm^{-1} indicates the presence of C–N stretching vibrations, possibly associated with amines. Finally, the peak at 496 cm^{-1} is consistent with C–H bending vibrations, reflecting the presence of aliphatic hydrocarbons.[42]

3.2 Optical characterization

Analysis of the as-synthesized carbon dots by UV-visible spectroscopy revealed distinct peaks (Fig. 2A). The UV-visible spectroscopy of the synthesized carbon dots reveals the presence of several absorbance peaks attributable to $\pi \rightarrow \pi^*$ and $n \rightarrow \pi^*$ electronic transitions originating from chromophores within the conjugated aromatic domains and surface functional groups decorating these CDs. Specifically, the 230 nm features suggest transitions associated with $\pi \rightarrow \pi^*$, while the 250 and 274 nm shoulder peaks correspond to $n \rightarrow \pi^*$ electronic transitions. Additionally, the broad peak at 365 nm and another at 474 nm indicate potential contributions from π–π^* transitions or the presence of conjugated structures and carbon nanodomain structures within the carbon dots.[38]

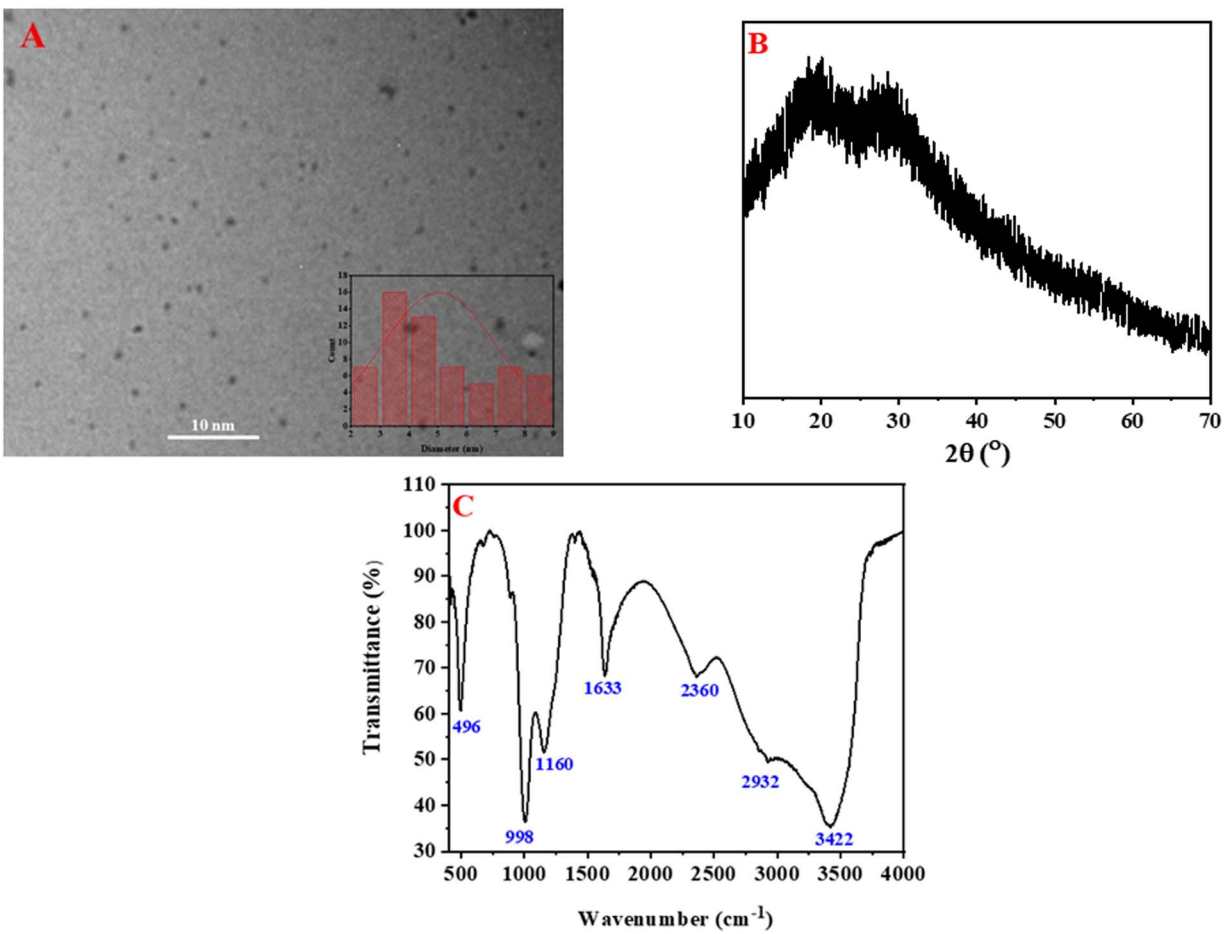

Fig. 1 (A) TEM image (inset: particle size distribution), (B) XRD pattern, and (C) FT-IR spectrum of DECDs.

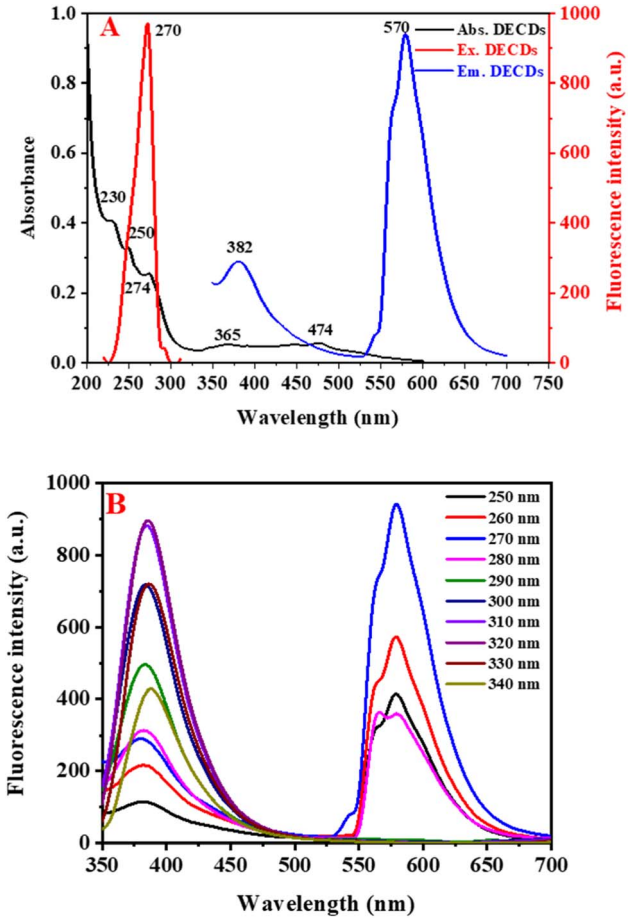

Fig. 2 (A) UV-visible absorption, fluorescence excitation, and emission spectra of the DECDs (1.0 mg mL^{-1}). (B) Emission spectra of the 1.0 mg mL^{-1} DECDs (1.0 mg mL^{-1}) at excitation wavelengths from 250 to 340 nm.

The plain DECDs exhibited an intrinsic fluorescence quantum yield of 18%. After doping the DECDs with a 0.1 mM solution of Co^{2+} ions, the fluorescence quantum yield was measured to be 25%. This signifies an enhancement of around 7% in the fluorescence efficiency of the DECDs upon incorporation of cobalt ions.

Fluorescence emission characterization of the carbon dots was performed under varied excitation wavelengths from 250 to 340 nm (Fig. 2B). Dual emission peaks centered at 382 nm and 570 nm were initially recorded with 270 nm photoexcitation. Tracking the emission while systematically tuning the excitation wavelength revealed dual fluorescence persisted from 250 to 280 nm excitations but only the shorter 382 nm peak remained above 280 nm. The 382 nm and 570 nm emission peaks demonstrated excitation-independent behavior. The dual fluorescence nature indicates that the 382 nm and 570 nm peaks arise from different emissive states within the carbon dots.[38] Likely the shorter wavelength peak corresponds to the surface defects or functional groups, while the longer 570 nm peak involves the carbon core structure.[38] Based on the excitation scanning, 270 nm excitation wavelength was optimal for concurrently maximizing both emissions at 382 nm and 570 nm.

3.3 Stability of DECDs

The influence of various conditions on the DECDs emission stability was examined to establish optimal assay conditions. The fluorescence signal at 382 nm is utilized as a reference signal to assess the fluorescence stability. Fluorescence spectra recorded over a wide pH range (2.0–10.0) showed consistent peak height between pH 5.0 to 10.0, with maximum intensity at neutral pH 7.0 in B.R. buffer (Fig. S1A†). However, acidic pH levels below 5.0 induced proton-mediated quenching, sharply diminishing dot emission.[43] The acidic environment causes the carbon dots to aggregate. This aggregation is a result of the increased proton concentration in acidic conditions, which can lead to changes in the surface chemistry and charge distribution of the carbon dots.[43] Additionally, high molar salt concentrations had negligible impact, as sodium chloride solutions up to 2.0 M did not significantly alter fluorescence response (Fig. S1B†). Prolonged direct UV irradiation for 5.0 h only slightly reduced intensities, confirming minimal susceptibility to photobleaching effect (Fig. S1C†).

3.4 Effects of experimental conditions on vancomycin detection

Optimal conditions were explored to achieve maximum sensitivity and fluorescence ratio F_{570}/F_{382} for vancomycin quantification through Co^{2+}-modulated carbon dot fluorescence quenching. The assay pH was systematically varied from 2.0 to 11.0 and the reaction equilibrium time studied from 0.5 to 10 minutes. Based on fluorescence stability spectra, a pH of 7 provided optimal carbon dot emission intensity and favorable Co^{2+}-vancomycin chelate formation kinetics near neutral conditions, without risk of Co^{2+} ion precipitation or antibiotic hydrolysis issues that can occur at pH extremes (Fig. S2A†). Reaction time testing showed fluorescent quenching reached completion within 1.0 minute (Fig. S2B†). Longer incubation periods up to 1.0 minutes revealed no further gains in quenching efficiency. Considering these assessments, B.R. buffer of pH 7.0 and 1.0 minute Co^{2+}-vancomycin reaction time were chosen as the ideal conditions that maximized detection sensitivity while ensuring stability, affinity, and rapid analysis. Different concentrations of $CoCl_2$ ranging from 0.01 to 1 mg mL^{-1} were tested. The fluorescence intensity of the DECDs was found to increase with increasing Co^{2+} concentration up to 0.1 mg mL^{-1}, beyond which it plateaued. Therefore, 0.1 mg mL^{-1} Co^{2+} was chosen as the optimal concentration to maximize fluorescence enhancement.

3.5 Ratiometric detection of vancomycin

Co@DECDs demonstrate two fluorescence peaks, characterized by maximum emission wavelengths at 382 nm and 570 nm. We examined the impact of different vancomycin concentrations on the fluorescence response of these two centers. As the vancomycin concentration increased, the fluorescence intensity of Co@DECDs system with at 382 nm gradually diminished, while the fluorescence intensity at 570 nm remained relatively unchanged (Fig. 3A). There is a good linear relationship

between vancomycin concentration and F_{570}/F_{382} (Fig. 3B). Their correlation in the range of 0.0–120.0 ng mL^{-1} was well fitted into a linear regression equation of $F_{570}/F_{382} = 0.011C_{(\text{vancomycin})} + 1.60$ ($R^2 = 0.9983$), indicating the superior ratiometric capability of Co@DECDs. Below 1 ng mL^{-1}, the changes were too small for reliable quantitative detection. Above 120 ng mL^{-1}, the response plateaued indicating saturation of the binding sites. The LOD of vancomycin was calculated to be around 0.31 ng mL^{-1} based on $3\sigma/s$ (where σ is the standard deviation of eight blank readings and s is the slope of the linearity curve). Co@DECDs demonstrate excellent ratiometric sensing capabilities for vancomycin detection when compared to other fluorometric methods reported in the literature (as summarized in Table 1). The proposed sensor exhibits a good linearity range and a relatively lower limit of detection (LOD), making it highly advantageous for accurate and sensitive vancomycin detection.

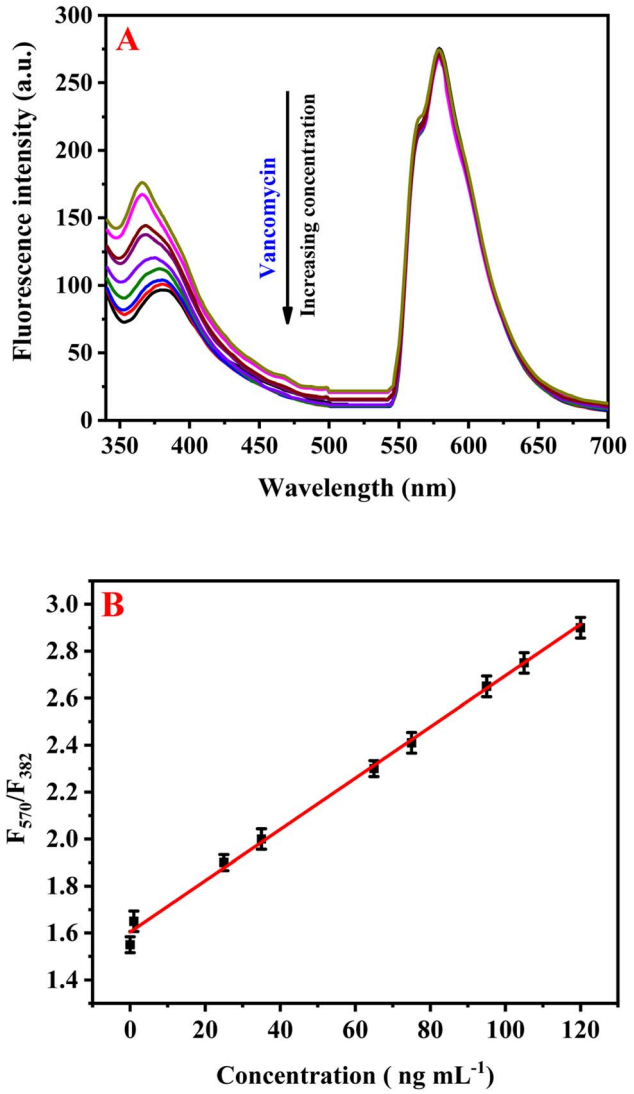

Fig. 3 (A) The effect of different concentrations of vancomycin (0.0–120.0 ng mL^{-1}) on the fluorescence intensity of Co@DECDs system. (B) Relationship of (F_{570}/F_{382}) *versus* vancomycin concentrations.

3.6 Selectivity

The selectivity of the Co@DECDs ratiometric sensor for vancomycin was examined by introducing various interferent species while monitoring the fluorescence emission ratio response to a 65.0 ng mL^{-1} standard vancomycin. The sensor tolerated high concentrations up to 600 ng mL^{-1} of biological ions like sodium, potassium, magnesium, carbonates and chloride, as well as urea, amino acids, and human serum albumin (HSA) with no discernible change in intensity ratios. The presence of other antibiotics like tetracycline, penicillin and erythromycin also produced negligible impacts (Fig. 4). Among all species screened, only vancomycin induced substantial increases in the fluorescence ratio (F_{570}/F_{382}) due to its specific chelation interactions with Co^{2+} ions integrated into the dot system. The highly selective response implies that the proposed sensor could be successfully applied for biological sample analysis. These results indicate that the ratiometric platform using Co@DECDs could provide reliable, robust detection for quality control and clinical drug monitoring.

3.7 Mechanism of detection

The synthesized DECDs displayed dual fluorescence emission peaks at 382 nm and 570 nm. Introduction of Co^{2+} ions amplified the fluorescence intensity at 382 nm, while the 570 nm peak remained unaltered. Subsequent addition of vancomycin induced quenching specifically at the 382 nm peak, indicating chelation interactions with Co^{2+} ions, while the 570 nm emission peak remained unchanged.

The mechanism of fluorescence enhancement of the DECDs in the presence of Co^{2+} ions was investigated by means of FT-IR, UV-vis, and fluorescence spectral measurements. As showed in Fig. 5 (A–C), UV-vis, fluorescence and FT-IR measurements of the DECDs show some changes after adding Co^{2+}.

FT-IR spectra of the DECDs before and after adding Co^{2+} ions were displayed in Fig. 5A. The shift in the broad O–H/N–H peak from 3422 cm^{-1} to 3405 cm^{-1}, accompanied by a narrower peak, suggests that the hydrogen-bonding environment around these groups has changed slightly upon addition of Co^{2+} ions. This could indicate coordination of Co^{2+} ions to oxygen or nitrogen donor atoms on the carbon dots. The small shift of the C–H peak from 2932 cm^{-1} to 2925 cm^{-1} may reflect minor conformational changes in the aliphatic hydrocarbons of the dot structure due to complexation with Co^{2+}. The lack of shift in the carbonyl and amine peaks suggests these moieties are likely not directly involved in binding to the Co^{2+} ions. These functional groups probably reside on the interior surface of the dots where they remain unaffected by Co^{2+} complexation events occurring within the exterior regions of the nanoparticles. The DECDs possessed surface functional groups such as amino and hydroxyl groups, which act as electron donors, as well as carboxyl groups, which act as electron acceptors. The presence of Co^{2+} ions caused chelation with the carboxyl groups on the DECDs' surfaces, thereby reducing their electron-accepting capability. This reduction in electron-accepting ability increased the likelihood of electron–hole recombination, ultimately leading to enhanced fluorescence emission.[44,45]

Table 1 Comparison of this work with other reported fluorescent probes for the detection of vancomycin

Probe	LOD (ng mL^{-1})	Linear range (ng mL^{-1})	Matrix	Ref.
Organic fluorescent probe	144.0	370–47520	Human serum	21
CdTe quantum dots	0.46	1.53–20000	Human serum	18
AuNCs	2.79	10–100000	Human serum	17
Ag-nanoparticles	0.29	1–36	Human plasma and urine	19
Coumarin/fluorescein	137.81	0–29700	Human serum and synthetic urine	22
Co@DECDs	0.31	1–120	Human plasma	This work

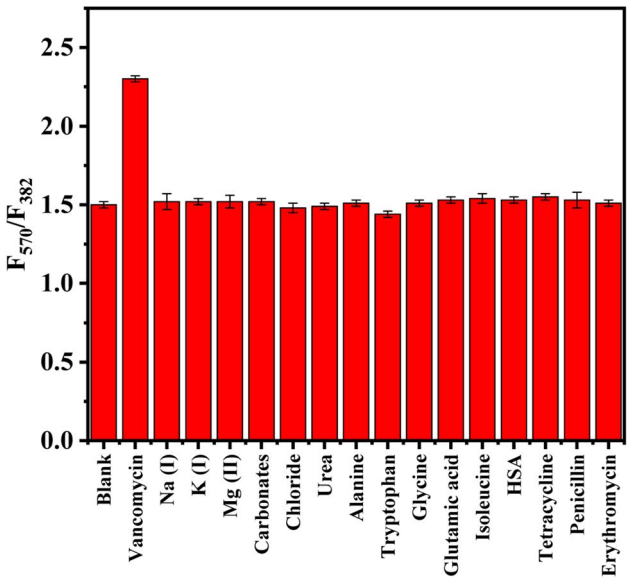

Fig. 4 The effect of different possible interferents (600.0 ng mL^{-1}) and vancomycin (65.0 ng mL^{-1}) on the fluorescence intensity ratio (F_{570}/F_{382}) of Co@DECDs system.

The UV-vis spectra of both the DECDs and the Co@DECDs system were examined, revealing notable changes upon the addition of Co^{2+} ions. The observed increase in absorption bands at 230 nm and 474 nm strongly suggests the formation of a complex between Co^{2+} ions and the carbon dots (Fig. 5B). The enhancement in absorbance at these specific wavelengths implies an altered electronic environment or energy state within the carbon dots due to the interaction with Co^{2+}ions. Such changes are indicative of complexation-induced modifications in the electronic structure of the carbon dots, supporting the formation of Co@DECDs system.[45]

As depicted in Fig. 5C, the fluorescence intensity of the DECDs is evident at 382 nm and 570 nm. Upon the introduction of Co^{2+} ions, the fluorescence at 382 nm undergoes a significant enhancement and a blue shift, providing additional confirmation of complex formation. Intriguingly, when vancomycin is introduced into the Co@DECDs solution, the initial fluorescence intensity of the DECDs is fully restored. This restoration is attributed to the complete release of Co^{2+} ions from the carbon dots, serving as compelling evidence that the DECDs are efficiently dissociated from the Co@DECDs complex in the presence of vancomycin. This observed fluorescence recovery further validates the reversible nature of the complexation and underscores the potential utility of vancomycin in modulating the interaction between DECDs and Co^{2+} ions.

For the binding interaction of Co@DECDs complex with vancomycin, the binding constants (K) and binding sites (n) were determined by the following equation:[46]

$$\log\left[\frac{F_0 - F}{F}\right] = \log\,[K] + n\log\,[Q]$$

F_0 is the fluorescence intensity without a quencher, F is the fluorescence intensity with the addition of a quencher, K is the corresponding binding constant, Q is the concentration of the quencher substance, and n is the number of binding sites. Where, K is the binding constant, that can be determined from the intercept of $\log\left[\frac{F_0 - F}{F}\right]$ *versus* $\log[Q]$ as shown in Fig. 5D. Thus, we obtained the following value for binding constant; $K = 8.92\ M^{-1}$ and number of binding sites (n) = 0.89. The value of "n" approximately equals to 1 indicates the existence of one binding site in vancomycin for cobalt ions in Co@DECDs system.

Experiments were done to address whether the DECDs without Co^{2+} can be applied for vancomycin detection or not. As shown in Fig. S3,† after addition of the vancomycin to the DECDs (without Co^{2+}), the intensity and shape of fluorescence spectrum were negligible. So, vancomycin had no interaction with the DECDs.

3.8 Analytical applications

The feasibility of using the proposed ratiometric fluorescence method for practical sample analysis was tested through vancomycin quantification experiments in spiked human blood plasma. The assay produced excellent recoveries (98.78–101.00%) of spiked concentrations across the tested concentrations, with standard deviations do not exceed 2.28% (Table 2). The excellent recovery values despite the complex plasma matrix components validate the reliability of the metal-modulated carbon dot sensor for biological samples applications. Success in directly detecting vancomycin without significant sample pre-processing steps also further confirms the strong selectivity mechanism and resistance to biological interferences.

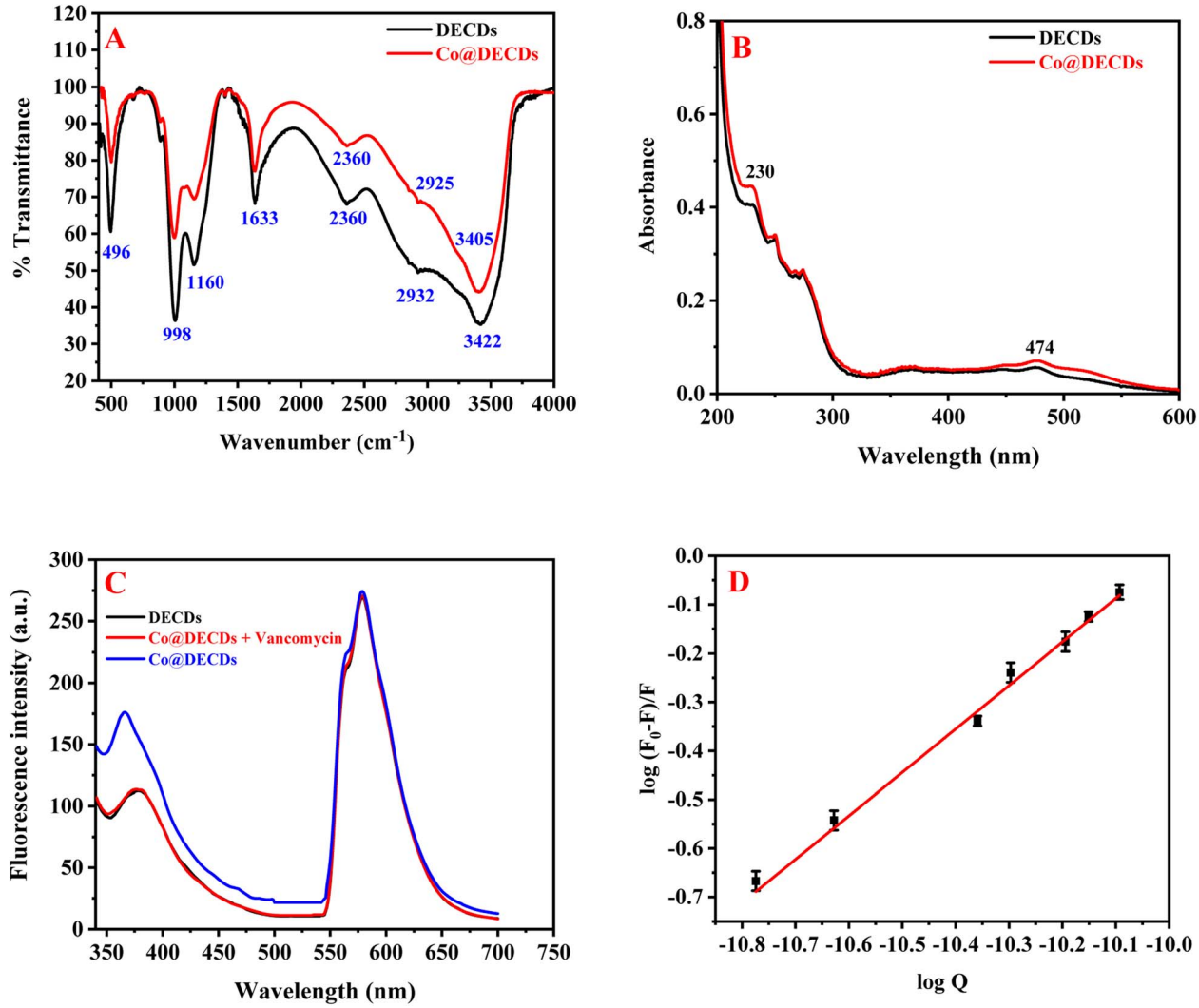

Fig. 5 (A) FT-IR spectral overlay of DECDs and Co@DECDs, (B) UV absorption spectra of DECDs and Co@DECDs, (C) emission spectra overlay of DECDs, Co@DECDs and Co@DECDs + vancomycin (120 ng mL^{-1}), (D) plot of log $\left[\frac{F_0 - F}{F}\right]$ *versus* log[*Q*].

Table 2 Detection of vancomycin in plasma samples ($n = 5$)

Added (ng mL^{-1})	Found (ng mL^{-1})	Recovery (%)	RSD (%)
1	1.01	101.00	1.25
25	25.24	100.96	2.28
35	34.89	99.69	0.89
65	64.21	98.78	1.002

4. Conclusions

In conclusion, this study presents a novel ratiometric fluorometric method for the quantification of vancomycin utilizing dual emissive carbon dots (DECDs) combined with Co^{2+} ions. The detection mechanism, including the interaction between vancomycin and Co^{2+} ions, was thoroughly investigated. The method demonstrated superior selectivity and simplicity compared to other fluorometric methods reported in the literature. The incorporation of Co^{2+} ions resulted in enhanced fluorescence intensity at 382 nm while maintaining a constant emission at 570 nm. The proposed method exhibited a good linearity and a sensitivity for vancomycin determination. Furthermore, the method showed high selectivity, as it successfully detected vancomycin in human plasma samples without interference from potential interfering species. While this method enables sensitive detection of vancomycin, the analysis was only demonstrated in spiked plasma samples. For practical applications, further clinical validation is required using real patient samples. This ratiometric fluorometric approach utilizing DECDs and Co^{2+} ions offers a promising and advantageous tool for sensitive and selective vancomycin detection in various clinical applications.

Conflicts of interest

The authors declare that they have no known competing financial interests or personal relationships that could have appeared to influence the work reported in this paper.

Acknowledgements

The authors would like to extend their appreciation to the Researchers Supporting Project number (RSPD2023R593) at King Saud University, Riyadh, Saudi Arabia.

References

1 M. J. Rybak, J. Le, T. P. Lodise, D. P. Levine, J. S. Bradley, C. Liu, B. A. Mueller, M. P. Pai, A. Wong-Beringer and J. C. Rotschafer, *Am. J. Health-Syst. Pharm.*, 2020, **77**, 835–864.
2 S. Elyasi, H. Khalili, S. Dashti-Khavidaki and A. Mohammadpour, *Eur. J. Clin. Pharmacol.*, 2012, **68**, 1243–1255.
3 V. Launay-Vacher, H. Izzedine, L. Mercadal and G. Deray, *Crit. Care*, 2002, **6**, 313–316.
4 M. T. Cafferkey, R. Hone and C. T. Keane, *J. Antimicrob. Chemother.*, 1982, **9**, 69–74.
5 M. J. Rybak, *Clin. Infect. Dis.*, 2006, **42**, S35–S39.
6 Y. Chu, Y. Luo, L. Qu, C. Zhao and M. Jiang, *Pharm. Biol.*, 2016, **54**, 2802–2806.
7 V. UshaVipinachandran, S. Rajendran, K. H. Badagoppam Haroon, I. Ashokan, A. Mondal and S. K. Bhunia, *ACS Appl. Nano Mater.*, 2020, **3**, 11659–11687.
8 T. Zhang, D. G. Watson, C. Azike, J. N. A. Tettey, A. T. Stearns, A. R. Binning and C. J. Payne, *J. Chromatogr. B*, 2007, **857**, 352–356.
9 M. Zamani-Kalajahi, S. Hamidi, M. Nemati and M. R. Siahi-Shadbad, *Instrum. Sci. Technol.*, 2024, **52**(1), 1–17.
10 M. Liu, Z.-H. Yang and G.-H. Li, *Molecules*, 2018, **23**, 2939.
11 M. Hadi and T. Mollaei, *Electroanalysis*, 2019, **31**, 1224–1228.
12 A. Blidar, B. Feier, A. Pusta, A.-M. Drăgan and C. Cristea, *Coatings*, 2019, **9**, 652.
13 B. Ackerman, H. Berg, R. Strate and J. Rotschafer, *J. Clin. Microbiol.*, 1983, **18**, 994–995.
14 K. B. Crossley, J. C. Rotschafer, M. M. Chern, K. E. Mead and D. E. Zaske, *Antimicrob. Agents Chemother.*, 1980, **17**, 654–657.
15 A. R. Júnior, M. M. D. C. Vila and M. Tubino, *Anal. Lett.*, 2008, **41**, 822–836.
16 H. A. El-Aziz, M. E. Fathy, N. El-Enany, F. A. Aly and M. M. Tolba, *Spectrochimica Acta, Part A*, 2021, **253**, 119570.
17 F. Mu, J. He, F. Fan and G. Shi, *Anal. Chim. Acta*, 2021, **1150**, 238177.
18 W. Liang, S. Liu, Z. Liu, D. Li, L. Wang, C. Hao and Y. He, *New J. Chem.*, 2015, **39**, 4774–4782.
19 A. R. Mohamed, *J. Fluoresc.*, 2022, **32**, 1899–1912.
20 Y. Oshima, M. Hori, M. Matsumoto and M. Kato, *AAPS Open*, 2023, **9**, 2.
21 S. M. Ng, X. Wu, M. F. Khyasudeen, P. J. Nowakowski, H.-S. Tan, B. Xing and E. K. L. Yeow, *ACS Sens.*, 2018, **3**, 1156–1163.
22 T. Deng, S. Hu, L. Zhao, S. Wu, W. Liu, T. Chen, T. Fu, H. Wang, H. Shi, X.-a. Huang and F. Liu, *Anal. Bioanal. Chem.*, 2019, **411**, 8103–8111.
23 M. K. Sharaf El-Din, F. Ibrahim, A. Kamal El-Deen and K. Shimizu, *J. Food Drug Anal.*, 2018, **26**, 834–841.
24 S. Rajendran, S. B. Zichri, V. Usha Vipinachandran, R. Jelinek and S. K. Bhunia, *ChemNanoMat*, 2021, **7**, 545–552.
25 E. Arad, S. K. Bhunia, J. Jopp, S. Kolusheva, H. Rapaport and R. Jelinek, *Adv. Ther.*, 2018, **1**, 1800006.
26 F. Belal, M. Mabrouk, S. Hammad, H. Ahmed and A. Barseem, *J. Fluoresc.*, 2023, **34**, 119–138.
27 G. Magdy, H. Elmansi, F. Belal and A. K. El-Deen, *Curr. Pharm. Des.*, 2023, **29**, 415–444.
28 S. A. Alkahtani, A. M. Mahmoud, Y. S. Alqahtani, A.-M. B. H. Ali and M. M. El-Wekil, *Spectrochim. Acta, Part A*, 2023, **303**, 123252.
29 A. H. Rageh, F. A. M. Abdel-aal, S. A. Farrag and A.-M. B. H. Ali, *Talanta*, 2024, **266**, 124950.
30 A.-M. B. H. Ali, F. A. M. Abdel-aal, A. H. Rageh and A.-M. I. Mohamed, *J. Sep. Sci.*, 2022, **45**, 4187–4197.
31 A. M. Mahmoud, S. A. Alkahtani, Y. S. Alqahtani, R. M. K. Mohamed, M. M. El-Wekil and A.-M. B. H. Ali, *Microchem. J.*, 2023, **194**, 109358.
32 S. K. Tammina, Y. Wan, Y. Li and Y. Yang, *J. Photochem. Photobiol., B*, 2020, **202**, 111734.
33 A. Z. Alanazi, K. Alhazzani, A. M. Mostafa, J. Barker, M. M. El-Wekil and A.-M. B. H. Ali, *J. Pharm. Biomed. Anal.*, 2024, **238**, 115862.
34 W. Lu, Y. Guo, J. Zhang, Y. Yue, L. Fan, F. Li, C. Dong and S. Shuang, *ACS Appl. Mater. Interfaces*, 2022, **14**, 57206–57214.
35 C. Hu, Y. Yin, C. Huang, Y. Dong, J. Liu, F. Xiao and S. Yang, *Microchem. J.*, 2024, **197**, 109735.
36 J. Raut, M. M. Islam, R. D. Sherpa, B. Sarkar, S. M. Mandal, S. P. Hui, S. Mandal and P. Sahoo, *Sci. Rep.*, 2022, **12**, 19366.
37 Y. Guo, X. Liu, C. Yang, X. Wang, D. Wang, A. Iqbal, W. Liu and W. Qin, *ChemCatChem*, 2015, **7**, 2467–2474.
38 S. Kainth, B. Maity, N. P. Shetti, S. Basu and R. R. Kakarla, *Nano Struct. Nano-Objects*, 2023, **33**, 100931.
39 A. Deb and D. Chowdhury, *Mater. Today Commun.*, 2022, **31**, 103777.
40 A.-M. I. Mohamed, N. A. Mohamed and A. M. B. H. Ali, *J. Planar Chromatogr.–Mod. TLC*, 2019, **32**, 285–294.
41 K. Alhazzani, A. Z. Alanazi, A. M. Mostafa, J. Barker, M. M. El-Wekil and H. A. A. M. Bellah, *RSC Adv.*, 2023, **13**, 28940–28950.
42 A. M. Mahmoud, S. S. Abu-Alrub, A. O. Alqarni, M. M. El-Wekil and A.-M. B. H. Ali, *Microchem. J.*, 2023, **191**, 108929.
43 S. Cao, X. Zhang, D. Xu, X. Fan, S. Mou, Y. Wang, N. Ye and W. Wang, *FEBS Lett.*, 2013, **587**, 1310–1315.
44 Y. Song, X. Xia, Z. Xiao, Y. Zhao, M. Yan, J. Li, H. Li and X. Liu, *J. Mol. Liq.*, 2022, **368**, 120663.
45 E. Mohagheghpour, L. Farzin, A. Ghoorchian, S. Sadjadi and M. Abdouss, *Spectrochim. Acta, Part A*, 2022, **279**, 121409.
46 D. Bharathi, R. H. Krishna, B. Siddlingeshwar, D. D. Divakar and A. A. Alkheraif, *J. Hazard. Mater.*, 2019, **369**, 17–24.